Journal of Photochemistry and Photobiology A: Chemistry 206 (2009) 205–212

Contents lists available at ScienceDirect

Journal of Photochemistry and Photobiology A: Chemistry

journal homepage: www.elsevier.com/locate/jphotochem

Magnetic field effect on chemical compositions of spherical Fe/Co fine particles synthesized from a gaseous mixture of iron pentacarbonyl and cobalt tricarbonyl nitrosyl

Hiroshi Morita[a,*], Anzu Kasai[b], Jan Šubrt[c], Zdeněk Bastl[d]

[a] Graduate School of Advanced Integration Science, Chiba University, Yayoi-cho, Inage-ku, Chiba 263-8522, Japan
[b] Graduate School of Science and Technology, Chiba University, Yayoi-cho, Inage-ku, Chiba 263-8522, Japan
[c] Institute of Inorganic Chemistry, Academy of Sciences of the Czech Republic, 25086 Řež near Prague, Czech Republic
[d] J. Heyrovský Institute of Physical Chemistry, Academy of Sciences of the Czech Republic, 18223 Prague, Czech Republic

ARTICLE INFO

Article history:
Received 30 April 2009
Received in revised form 15 June 2009
Accepted 3 July 2009

Keywords:
Gas phase photochemical reaction
Aerosol particle
Particle wire
Magnetic field effect
Iron pentacarbonyl
Cobalt tricarbonyl nitrosyl

ABSTRACT

Under UV light irradiation on a gaseous mixture of $Fe(CO)_5$ and $Co(CO)_3NO$, both the crystalline deposits with sizes of ~5 and ~18 μm and the spherical particles with a mean diameter of 0.3 μm were produced. From FT-IR spectra and SEM–EDS analysis, it was suggested that the chemical structure of the crystalline deposits was the one of $Fe_2(CO)_9$ being modified by involving Fe—(C=O)—Co bond. By decreasing a partial pressure of $Fe(CO)_5$ to 0.5 Torr in the gaseous mixture, only the spherical aerosol particles could be produced. Chemical composition of the particles was rich in Co species. From the disappearance of bridging C=O band in the FT-IR spectra of the particles and the appearance of C—O bands coordinated to a metal atom, Fe atom in $Fe(CO)_4$ was suggested to be coordinated by the O atom in bridging C=O bond in Co—(C=O)—Co structure and/or in α-diketone structure which was formed from two CO groups in dicobalt species. Chemical compositions of the crystalline deposits and the spherical particles were influenced differently by the application of a magnetic field. Atomic ratio of Fe to Co atom decreased in the crystalline deposits whereas it increased in the spherical particles with increasing magnetic field up to 5 T. Linearly aggregated particles (i.e., particle wires) as long as 30 μm were produced on the front side of a glass plate placed at the bottom of the irradiation cell.

1. Introduction

Under light irradiation, iron pentacarbonyl ($Fe(CO)_5$) evolves CO species to produce $Fe(CO)_4$ followed by the formation of $Fe_2(CO)_9$ and $Fe_3(CO)_{12}$ [1–4]. By chemical vapor deposition (CVD) with the aid of CO_2 laser pyrolysis, $Fe(CO)_5$ produced Fe_2O_3 [5,6], γ-Fe [7], and α-Fe nanoparticles [8,9] depending on different experimental conditions. Through the interaction with cobalt tricarbonyl nitrosyl ($Co(CO)_3NO$), $Fe(CO)_5$ produced γ-Fe–Co alloy via dielectric breakdown with CO_2 laser pyrolysis [10] and $CoFe_2O_4$ particles under sonochemical decomposition [11].

In order to produce spherical particles, we have developed a photochemical method where photochemical reactions of reactive molecules were used to initiate nucleation reaction during aerosol particle formation [12–16]. Using the photochemical method, spherical particles involving organometal compounds were successfully produced from gaseous mixtures of $Fe(CO)_5$ and carbon disulfide (CS_2) [17,18], $Fe(CO)_5$ and allyltrimethylsilane (ATMeSi) [19], $Co(CO)_3NO$ and CS_2 [20], and $Co(CO)_3NO$ and ATMeSi [21]. Particle size was effectively diminished by shortening the irradiation time of UV light and particles as small as 58 nm was produced from a gaseous mixture of $Fe(CO)_5$ and CS_2 [18]. Furthermore, the chemical composition of the particles was changed by the application of a magnetic field during UV light irradiation [17,20]. The photochemical method thus developed showed several advantages in producing spherical aerosol particles [22].

In the present study, we have tried to produce aerosol particles involving Fe and Co species from a gaseous mixture of $Fe(CO)_5$ and $Co(CO)_3NO$ by using the photochemical method. Morphology of the crystalline deposits was changed to the spherical particles by controlling the partial pressure of $Fe(CO)_5$, and the magnetic field effect on the chemical compositions of the products was investigated by measuring scanning electron microscopy/energy dispersive spectroscopy (SEM–EDS) and X-ray photoelectron spectra (XPS). Chemical structure of the spherical particles was briefly discussed based on FT-IR spectra.

* Corresponding author. Tel.: +81 50 1332 5434; fax: +81 43 432 1168.
E-mail address: hmorita@faculty.chiba-u.jp (H. Morita).

1010-6030/$ – see front matter © 2009 Elsevier B.V. All rights reserved.
doi:10.1016/j.jphotochem.2009.07.004

2. Experimental

$Fe(CO)_5$ (Kanto, 95%) and $Co(CO)_3NO$ (Gelest, 95%) were degassed by freeze-pump-thaw cycles in the dark and purified by vacuum distillation immediately before use. A gaseous mixture of $Fe(CO)_5$ and $Co(CO)_3NO$ was prepared by two procedures. In the first, each vapor was introduced successively into a cross-shaped Pyrex cell having a long (length 155 mm, inner diameter 35 mm) and short (length 80 mm, inner diameter 20 mm) arms or into a small cylindrical Pyrex cell (length 160 mm, inner diameter 20 mm, volume 50 cm^3) equipped with a couple of quartz windows through a vacuum line equipped with a capacitance manometer (Edwards Barocel Type 600). In the second procedure, a fixed amount of $Co(CO)_3NO$ vapor which was first introduced into the irradiation cell was collected into a glass tube by freezing with liquid nitrogen. Then, $Fe(CO)_5$ vapor was introduced into the irradiation cell through the vacuum line, followed by the introduction of $Co(CO)_3NO$ vapor which had already been trapped in the glass tube. The background pressure of the irradiation cell was less than 1×10^{-4} Torr (1 Torr = 133.3 Pa). The partial pressures of $Fe(CO)_5$ and $Co(CO)_3NO$ in the irradiation cell were determined from the diagnostic band intensities of FT-IR spectra at 645 cm^{-1} for $Fe(CO)_5$ and 2108 cm^{-1} for $Co(CO)_3NO$. The gaseous samples were irradiated with a medium pressure mercury lamp (Ushio UM-452, 450W) through UV29 and UV-D33S filters (energy, 5.4 mJ/s cm^2) to excite both $Fe(CO)_5$ and $Co(CO)_3NO$ molecules at 313 and 365 nm. Light intensity at 365 nm was 1.6 times stronger than the one at 313 nm. Absorbance of 1 Torr of $Fe(CO)_5$ and of $Co(CO)_3NO$ is 0.28 and 0.06, respectively, at 313 nm, and 0.06 and 0.23, respectively, at 365 nm in 10 cm light path length. Monitor (He–Ne laser) light intensity scattered by the aerosol particles as formed in the irradiation cell during UV light irradiation was measured with a combination of a photomultiplier tube (EMI 6256S) and a lock-in amplifier (SRS SR-530) through a Y-52 filter. Both the crystalline deposits and sedimentary particles were deposited on a glass plate and/or Cu substrate placed at the bottom of the irradiation cell.

Scanning electron microscope (SEM) images were recorded with a JEOL JSM 6060 scanning electron microscope, and SEM–EDS analyses were performed using a Philips XL30 CP EDAX scanning electron microscope. XPS of deposits were measured with a Gammadata Scienta ESCA 310 electron spectrometer using monochromatized Mg Kα radiation for electron excitation. The crystalline deposits and sedimentary particles were mixed with KBr powder to prepare KBr pellets and FT-IR spectra of the deposits embedded in the pellets were measured with a Nicolet NEXUS 470 FT-IR spectrometer. Magnetic field was applied by a helium-free superconducting magnet (Toshiba TM-5SP).

3. Results and discussion

3.1. Chemical structure of deposits produced from a $Fe(CO)_5/Co(CO)_3NO$ gaseous mixture

Under UV light irradiation with a medium pressure mercury lamp at 313 and 365 nm for 30 min, a gaseous mixture of $Fe(CO)_5$ (2.3 Torr) and $Co(CO)_3NO$ (1.7 Torr) produced crystalline deposits with sizes of 13–25 μm (mean size 18 μm) and of ~5 μm in addition to a small amount of spherical sedimentary particles with a mean diameter of 0.42 μm as shown in Fig. 1(a). The morphology of the deposits was different from that deposited from pure $Co(CO)_3NO$ vapor. $Co(CO)_3NO$ vapor at a pressure of 2 Torr produced coagulated sedimentary particles with a mean diameter of 82 nm (Fig. 1(b)) under light irradiation for 60 min. As was reported previously [17], $Fe(CO)_5$ produced two kinds of crystalline deposits composed of $Fe_2(CO)_9$ and $Fe_3(CO)_{12}$. The crystalline deposits from the gaseous mixture may originate mainly from $Fe(CO)_5$.

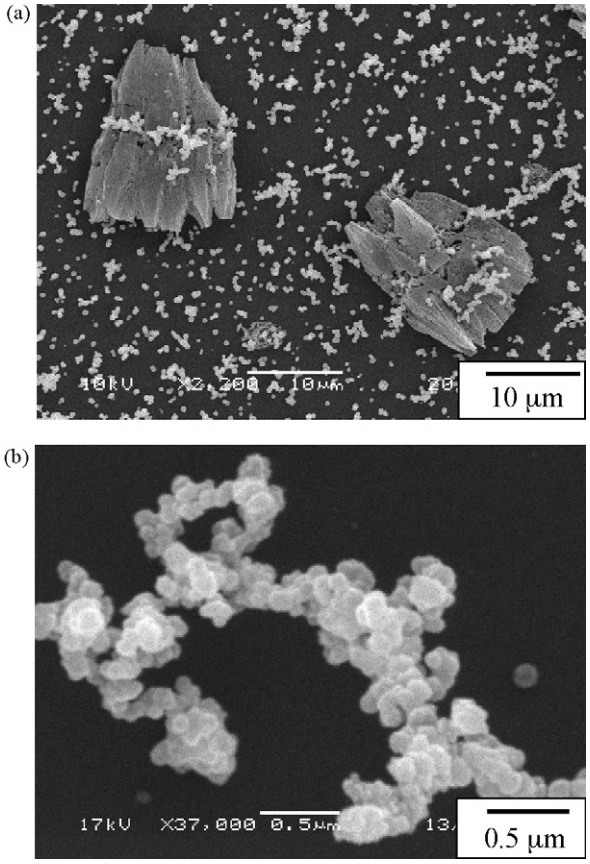

Fig. 1. SEM images of deposits produced from (a) a gaseous mixture of $Fe(CO)_5$ (2.3 Torr) and $Co(CO)_3NO$ (1.7 Torr) and (b) pure $Co(CO)_3NO$ vapor (2.0 Torr) under light irradiation with a medium pressure mercury lamp for (a) 30 min and (b) 1 h. Original magnification of SEM, (a) 2200×, (b) 37,000×.

Dependence of morphological change of the crystalline deposits on light irradiation time was studied. During light irradiation for 2 min, only sedimentary particles with a mean diameter of 0.26 μm were detected as shown in Fig. 2A(a). The sedimentary particles had a tendency to coagulate in each other. At several spots, many particles were accumulated to form islands of several μm in size (Fig. 2A(b)). After light irradiation for 5 min, crystalline deposits with a size of 5–10 μm were observed in addition to spherical particles with a mean diameter of 0.27 μm (Fig. 2B). During prolonged light irradiation up to for 30 min, crystalline deposits with sizes of ~18 μm were formed in addition to crystalline deposits of ~5 μm in size and sedimentary particles as shown in Fig. 1(a). It is clear that crystalline deposits grow up separately from spherical particles under prolonged light irradiation.

FT-IR spectra of the deposits are shown in Fig. 3, compared with the spectra of deposits produced from pure $Fe(CO)_5$ and $Co(CO)_3NO$ vapors. The spectrum of sedimentary particles deposited from the gaseous mixture over 2 min under light irradiation was different from the spectra of deposits produced over 5 and 30 min under light irradiation in that chemical species originating from $Co(CO)_3NO$ were involved significantly. The spectral features of deposits under light irradiation over 30 min practically coincided with those of the deposits produced from pure $Fe(CO)_5$ vapor (Fig. 3(e)) which were assigned to $Fe_2(CO)_9$ [2,3]. This reflected the fact that the product yield of the crystalline deposits was much higher than that of the particles and the main chemical component of the crystalline deposits was similar to that of $Fe_2(CO)_9$.

From SEM–EDS analysis, incorporation of $Co(CO)_3NO$ into the crystalline deposit was investigated. The population of Fe, Co, C,

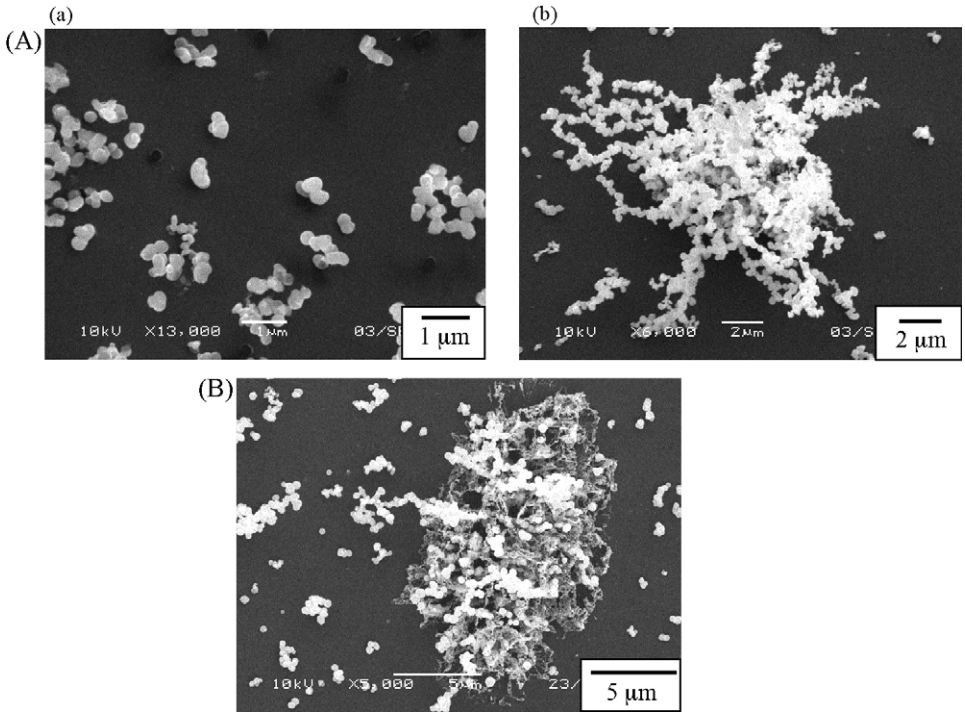

Fig. 2. SEM images of deposits produced from a gaseous mixture of $Fe(CO)_5$ (2.3 Torr) and $Co(CO)_3NO$ (1.7 Torr) under light irradiation with a medium pressure mercury lamp for (A) 2 and (B) 5 min. Original magnification of SEM, (A) (a) 13,000×, (b) 6000×, (B) 5000×.

and O atoms in the crystalline deposits produced from a gaseous mixture of $Fe(CO)_5$ (2.4 Torr) and $Co(CO)_3NO$ (1.3 Torr) is tabulated in Table 1. The atomic ratio of Co atom to Fe atom was 1:13, showing that $Co(CO)_3NO$ molecules were actually incorporated into the formation process of the crystalline deposits. It is strongly suggested that the chemical structure of the crystalline deposits is the one of $Fe_2(CO)_9$ being modified by involving Fe—(C═O)—Co bond.

The nucleation and propagation processes during aerosol particle formation were monitored by measuring the He—Ne laser light intensity scattered by the aerosol particles which were formed under UV light irradiation. The results are shown in Fig. 4. Compared with the cases of pure $Fe(CO)_5$ vapor (1.0 Torr) and pure $Co(CO)_3NO$ (2 Torr) where the nucleation and propagation reactions were fast and the scattered light was detected only for the first 1 min and 4 min, respectively, scattered light was detected for the first 15 min for the gaseous mixture of $Fe(CO)_5$ (2.3 Torr) and $Co(CO)_3NO$ (1.7 Torr), showing that the aerosol particles were actually formed by the chemical reaction between $Fe(CO)_5$ and $Co(CO)_3NO$ molecules. Incorporation of $Co(CO)_3NO$ molecules decelerated the formation of $Fe_2(CO)_9$.

Chemical processes in the gas phase were investigated by measuring FT-IR spectrum of a gaseous mixture of $Fe(CO)_5$ (2.3 Torr) and $Co(CO)_3NO$ (1.7 Torr). The spectra of $Fe(CO)_5$ vapor (2 Torr) and $Co(CO)_3NO$ vapor (2 Torr) are shown in Fig. 5A. Upon UV light exposure, FT-IR bands of $Fe(CO)_5$ and $Co(CO)_3NO$ decreased their intensities both in pure vapors and in the gaseous mixture. After allowing for complete sedimentation of the formed aerosol particles, the band intensity (absorbance, A) of δ(Fe—C—O) band at 645 cm^{-1} of $Fe(CO)_5$ [23,24] and of ν(C≡O) band at 2108 cm^{-1} of $Co(CO)_3NO$ [25,26] was measured, and the value, A/A_0, was plotted against cumulative irradiation time (Fig. 5B). In pure vapor, $Fe(CO)_5$ molecules were almost completely consumed in 10 min, whereas in the gaseous mixture, they still remained by ~17% even after 60 min. On the other hand, $Co(CO)_3NO$ molecules were consumed by only ~20% during 60 min under light irradiation both in pure vapor and in the gaseous mixture. Assuming the pseudo first order decay, the depletion rate was estimated; depletion of $Fe(CO)_5$ molecules was decelerated by ≈6 times due to the presence of $Co(CO)_3NO$. In contrast to this, the depletion rate of $Co(CO)_3NO$ molecules is only slightly (1.4 times) increased in the gaseous mixture.

The number of molecules depleted from the gaseous phase was estimated. In the gaseous mixture, molar ratio of depleted $Fe(CO)_5$ and $Co(CO)_3NO$ molecules over 3 min under UV light irradiation was ~3.6. After 40 min under UV light irradiation, the molar ratio of depleted molecules increased to ~5.0 due to the formation of crystalline deposit besides the particle formation.

Table 1
Atomic abundance of Fe and Co atoms in crystalline deposits produced from a gaseous mixture of $Fe(CO)_5$ (2.4 Torr) and $Co(CO)_3NO$ (1.3 Torr) under a magnetic field of 0 and 5 T.

Atomic line	Magnetic field			
	0 T		5 T	
	At %	Ratio	At %	Ratio
Fe K	24.8	1	21.8	1
Co K	1.9	0.075	2.7	0.13
C K	23.6	0.95	29.2	1.34
O K	49.7	2.00	46.2	2.12

3.2. *Magnetic field effect on chemical compositions of deposits produced from a $Fe(CO)_5/Co(CO)_3NO$ gaseous mixture*

Magnetic field effects on both the morphology and the chemical compositions of the crystalline deposits and the sedimentary aerosol particles were investigated from SEM images and SEM–EDS and XPS analyses. Crystalline deposits and spherical particles with a mean diameter of ~0.2 μm were produced from a gaseous mixture of $Fe(CO)_5$ (2.4 Torr) and $Co(CO)_3NO$ (1.3 Torr) in a superconducting magnet using a cylindrical cell with an inner diameter of 20 mm under light irradiation for 60 min. Use of a smaller irradiation cell resulted in the decrease of the mean diameter of the sedimentary particles [18]. SEM images of the crystalline deposits are shown in

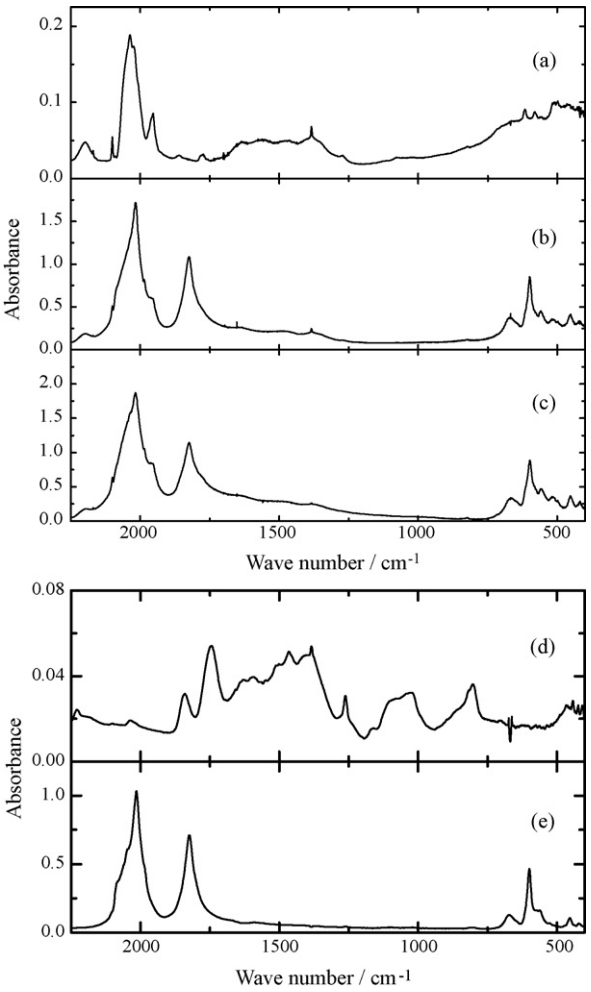

Fig. 3. FT-IR spectra of deposits produced from a gaseous mixture of $Fe(CO)_5$ (2.3 Torr) and $Co(CO)_3NO$ (1.7 Torr) under light irradiation for (a) 2, (b) 5, and (c) 30 min, and those produced from (d) pure $Co(CO)_3NO$ vapor (2.0 Torr) and (e) pure $Fe(CO)_5$ vapor (1.0 Torr) under light irradiation for (d) 1 h and (e)10 min.

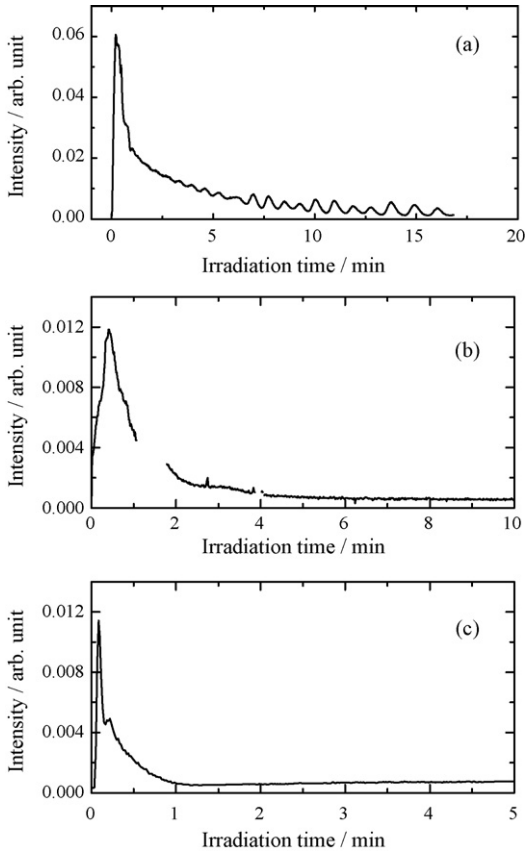

Fig. 4. He–Ne laser light intensity scattered by aerosol particles produced from (a) a gaseous mixture of $Fe(CO)_5$ (2.3 Torr) and $Co(CO)_3NO$ (1.7 Torr), (b) pure $Co(CO)_3NO$ vapor (2.0 Torr) and (c) pure $Fe(CO)_5$ vapor (1.0 Torr) under light irradiation with a medium pressure mercury lamp.

Fig. 6. In the absence of an external magnetic field, the crystalline deposits with a size of ~5 μm were produced. Under a magnetic field of 3 T, the crystalline deposits grew vertically onto a substrate placed at the bottom of the irradiation cell and had a shape like a rose petal. At 5 T, the deposits became larger and more dense and had a hexagonal shape lying down on the substrate. The morphological change of the deposits strongly suggested that the formation process of the crystalline deposits was accelerated by the application of a magnetic field. SEM–EDS analysis was performed on the spherical particles and on the crystalline deposits separately, and the results are tabulated in Table 2. The atomic ratio of Fe to Co atom was 13 for the crystalline deposits and 1.8 for the particles. Co species were relatively rich in the particles. Different chemical compositions between the crystalline deposits and the particles supported for the suggestion in Fig. 2 that the crystalline deposits were formed independently from the spherical particles. This was further supported from different magnetic field effect on the crystalline deposits and the particles tabulated in Table 2. With increasing magnetic field, Co species increased in the crystalline deposits, whereas Fe species increased in the particles.

Table 2
Atomic ratio of Fe to Co atom in sedimentary particles and in crystalline deposits produced from a gaseous mixture of $Fe(CO)_5$ (2.4 Torr) and $Co(CO)_3NO$ (1.3 Torr) under a magnetic field.

	Magnetic field			
	0 T	3 T	4 T	5 T
Particles	1.8	1.7	2.5	2.5
Crystalline deposit	13	12	12	8.6

Under UV light irradiation, $Fe(CO)_5$ and $Co(CO)_3NO$ evolve CO and/or NO groups to produce reactive species (reactions (1)–(3)) [27–29].

$$Fe(CO)_5 + h\nu \rightarrow Fe(CO)_4 + CO \quad (1)$$

$$Co(CO)_3NO + h\nu \rightarrow Co(CO)_3 + NO \quad (2)$$

$$Co(CO)_3NO + h\nu \rightarrow Co(CO)_2NO + CO \quad (3)$$

In the gaseous mixture, $Fe(CO)_4$ reacts with $Fe(CO)_5$ and $Co(CO)_3NO$ to form the crystalline deposits involving Fe—(C=O)—Co bond (reactions (4) and (5)).

$$Fe(CO)_4 + Fe(CO)_5 \rightarrow Fe_2(CO)_9 \quad (4)$$

$$Fe(CO)_4 + Co(CO)_3NO \rightarrow FeCo(CO)_7NO \quad (5)$$

$Co(CO)_3$ may react with $Fe_2(CO)_9$ to form any chemical species involving Fe and Co atoms (reaction (6)).

$$Co(CO)_3 + Fe_2(CO)_9 \rightarrow \text{chemical species involving Co and Fe atoms (such as } Fe_2Co(CO)_{12}) \quad (6)$$

As for the particle formation, $Co(CO)_3$ reacts with $Co(CO)_3NO$ to form any reactive species such as $Co_2(CO)_6NO$ to initiate the nucleation reaction (reaction (7)). These dicobalt species may react with

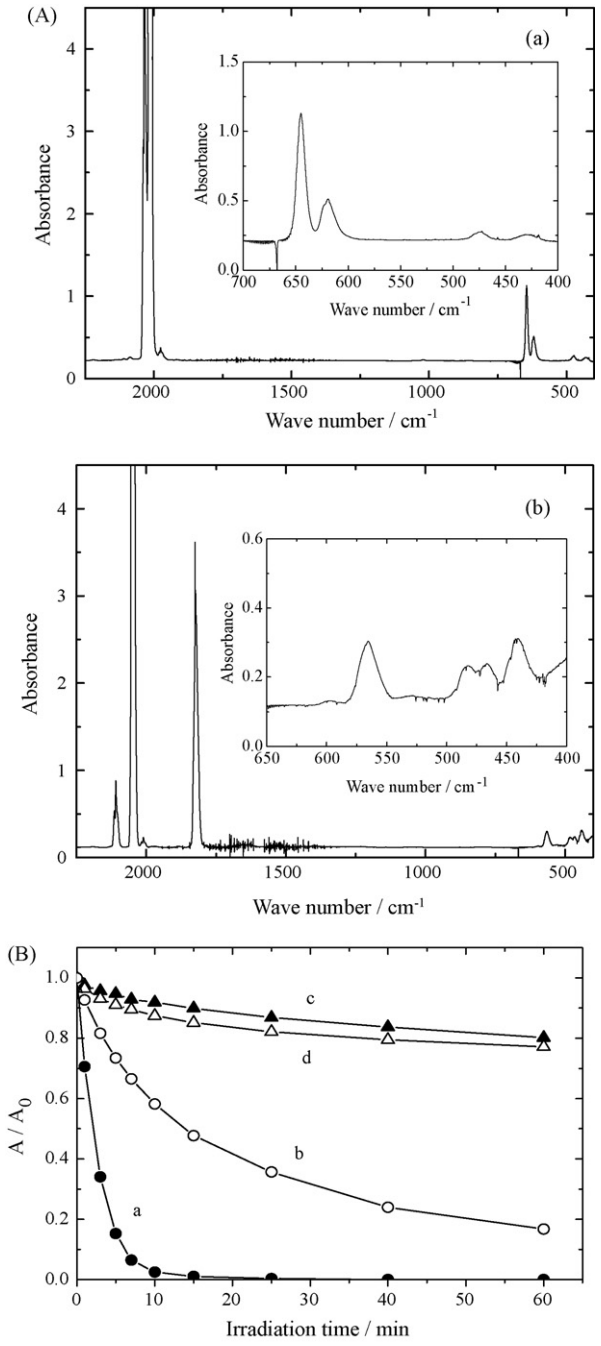

Fig. 5. (A) FT-IR spectra of (a) pure $Fe(CO)_5$ vapor (2.0 Torr) and (b) pure $Co(CO)_3NO$ vapor (2.0 Torr). (B) Depletion (A/A_0) of δ(Fe—C—O) band of $Fe(CO)_5$ in (a) pure $Fe(CO)_5$ vapor (2.0 Torr) and (b) a gaseous mixture of $Fe(CO)_5$ (2.3 Torr) and $Co(CO)_3NO$ (1.7 Torr) and depletion of ν(C≡O) band of $Co(CO)_3NO$ in (c) pure $Co(CO)_3NO$ vapor (2.0 Torr) and (d) a gaseous mixture of $Fe(CO)_5$ (2.3 Torr) and $Co(CO)_3NO$ (1.7 Torr) against irradiation time.

$Fe(CO)_5$ and $Fe(CO)_4$ to form chemical species involving Co and Fe atoms (reaction (8)).

$$Co(CO)_3 + Co(CO)_3NO \rightarrow Co_2(CO)_6NO \quad (7)$$

$$Co_2(CO)_6NO + Fe(CO)_5 \text{ and/or } Fe(CO)_4 \rightarrow \text{chemicalspeciesinvolvingCoandFeatoms} \quad (8)$$

Judging from the magnetic field dependency on the chemical compositions analyzed by SEM–EDS (Table 2), reactions (6) and (8) may be accelerated by the magnetic field to result in the increase in atomic abundance of Co atom in the crystalline deposits and Fe atom in the sedimentary particles. Acceleration of reaction (6) may be responsible also to the morphological change of the crystalline deposits.

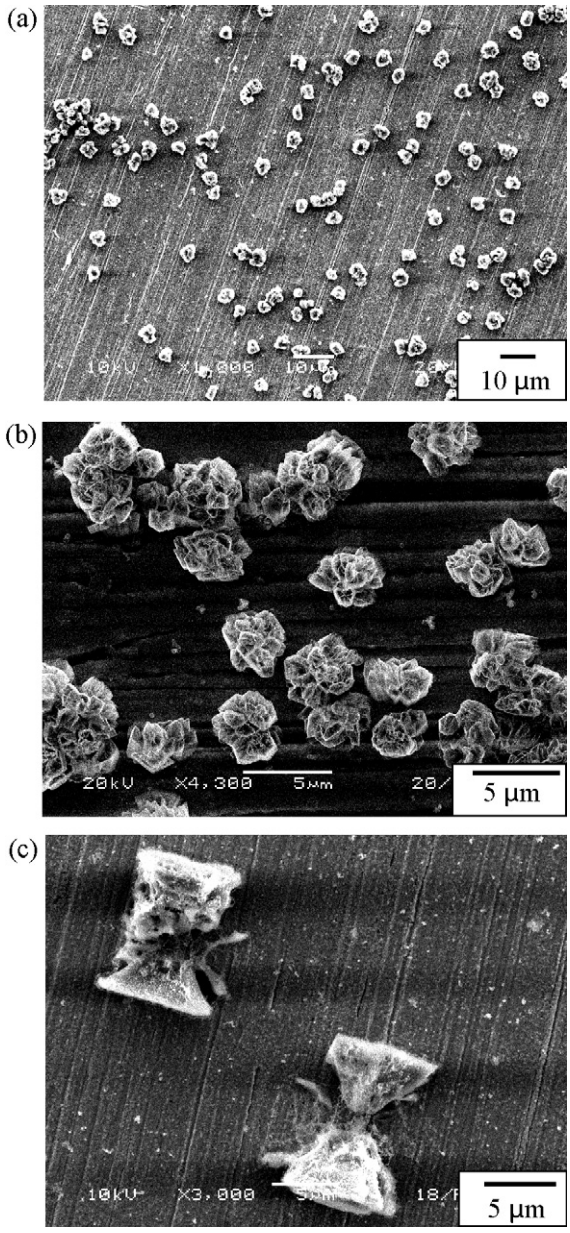

Fig. 6. SEM images of deposits produced from a gaseous mixture of $Fe(CO)_5$ (2.4 Torr) and $Co(CO)_3NO$ (1.3 Torr) under light irradiation with a medium pressure mercury lamp for 60 min under a magnetic field of (a) 0, (b) 3, and (c) 5 T. Original magnification of SEM, (a) 1000×, (b) 4300×, (c) 3000×.

Under a magnetic field of 5 T, the crystalline deposits had a hexagonal shape and the long axis of the crystalline deposits was aligned perpendicularly to the applied magnetic field as was reported previously [30]. The mass magnetic susceptibility was determined to be $(7.0 \mp 1.9) \times 10^{-9}\ m^3\ kg^{-1}$, and showed that the crystalline deposits were paramagnetic. To study the chemical structure in more detail, XPS were measured with the crystalline deposits. The spectra are shown in Fig. 7. In the spectra, Fe $2p_{3/2}$ electrons were detected at a binding energy of 710.7 eV. The measured binding energy as well as the energy separation between Fe $2p_{3/2}$ line and a satellite was characteristic of Fe^{3+} species. Co $2p_{3/2}$ and Co $2p_{1/2}$ electrons were detected at binding energies of 780.8

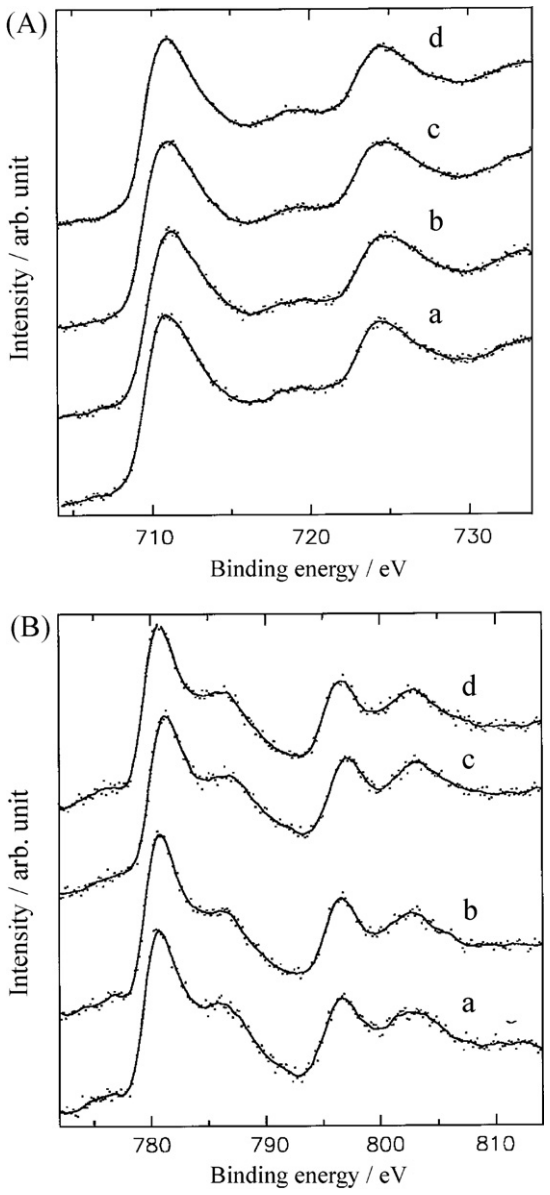

Fig. 7. XPS of (A) Fe 2p and (B) Co 2p electrons of crystalline deposits produced from a gaseous mixture of $Fe(CO)_5$ (2.4 Torr) and $Co(CO)_3NO$ (1.3 Torr) under light irradiation for 60 min with the application of a magnetic field of (a) 0, (b) 3, (c) 4, and (d) 5 T.

and 796.6 eV with satellite structure. The spectrum was characteristic of divalent paramagnetic Co^{2+}, indicating that Co species gave the paramagnetic characters to the deposits. The stoichiometry of Fe and Co atoms was 1.0: 0.40, 1.0: 0.49, 1.0: 0.50, and 1.0: 0.45 for the deposits produced under a magnetic field of 0, 3, 4, and 5 T, respectively. The ratio of Fe to Co atom was largely different from the value analyzed by SEM–EDS in Table 2. This was due partly to a shallower measuring depth of XPS than SEM–EDS, suggesting that Co atoms were more abundant in the surface region of the crystalline deposits. Although the XPS analysis involved a minor contribution from the particles, the crystalline deposits increased the contribution of Co atoms under the magnetic field, being consistent with the result of SEM–EDS analysis.

3.3. Formation and chemical structure of spherical aerosol particles

As discussed above, a gaseous mixture which contained more $Fe(CO)_5$ vapor (2.3 Torr) than $Co(CO)_3NO$ vapor (1.7 Torr) produced both the crystalline deposits and the sedimentary spherical particles. The crystalline deposits were rich in Fe species and were produced after the deposition of the particles. These experimental results strongly suggest that in order to produce the particles predominantly by suppressing the formation of the crystalline deposits, a decrease in the partial pressure of $Fe(CO)_5$ is effective. Hence, the partial pressure of $Fe(CO)_5$ was decreased to 0.4 Torr, and a gaseous mixture of $Fe(CO)_5$ (0.4 Torr) and $Co(CO)_3NO$ (2.4 Torr) was irradiated with UV light for 7 and 60 min, resulting in the production of only sedimentary aerosol particles with a mean diameter of 0.31 and 0.39 μm, respectively as shown in Fig. 8A. Monitor (He–Ne laser) light scattered by the aerosol particles was detected only for the first 20 min (Fig. 9). This showed that aerosol particles were formed during the first 20 min. The crystalline deposits were not formed until 60 min after the particle formation under the present experimental conditions.

It is worth mentioning that during the deposition of aerosol particles, linearly aggregated particles (i.e., particle wires) as long as 30 μm were produced on the front side of a glass plate (placed at the bottom of the irradiation cell). Particle wires were deposited on the surface of the glass plate or accumulating into the space (Fig. 8B). The production of the particle wires is characteristic of the aerosol particles synthesized by the photochemical method [21,22]. Under some experimental conditions, light irradiation can induce a modulated convectional flow of the entire gaseous sample to result in a deposition of particles linearly aggregated in each other. Because the sedimentary particles maintain the photochemical reactivity even after depositing on a substrate, two neighboring particles can be connected in each other via chemical reaction. The production of particle wires is an advantage of the photochemical method [22].

Chemical structure and chemical composition of the spherical particles were studied by measuring SEM–EDS and FT-IR spectra. SEM–EDS analysis was performed on the sedimentary particles produced from a gaseous mixture of $Fe(CO)_5$ (0.4 Torr) and $Co(CO)_3NO$ (2.6 Torr). Because the signals from uncovered Cu substrate were intense, signals from Fe and Co atoms became relatively weak. The results are tabulated in Table 3. Atomic ratio of Fe to Co atom was 1:1.5, revealing that chemical composition of the particles was rich in Co species. FT-IR spectrum of the sedimentary aerosol particles is shown in Fig. 10. The spectrum showed strong bands at 1955, 2025, 2052, 2100, and 2198 cm^{-1} assigned to terminal CO stretching vibration of Co and Fe species [23–26,31], and bands in the 1250–1650 cm^{-1} region (at 1384, 1470, 1495, and 1633 cm^{-1}) which were characteristic of the deposits from $Co(CO)_3NO$ and were assignable to C—O bond coordinated to a metal atom. In the spherical particles, IR bands ascribed to bridging C═O (at 1825 cm^{-1} in Fig. 3(b)) and terminal NO (at 1822 cm^{-1} in Fig. 5A(b)) [26] disappeared almost completely. Chemical structure is suggested to be entirely different from that of the crystalline deposits shown in Fig. 3(b) which are mainly composed of $Fe_2(CO)_9$ structure involving Fe—(CO)—Co bond. In the particles, Co species are more abundant than Fe species. Co atoms can be connected

Table 3
Atomic abundance of Fe and Co atoms in sedimentary aerosol particles produced from a gaseous mixture of $Fe(CO)_5$ (0.4 Torr) and $Co(CO)_3NO$ (2.6 Torr) under a magnetic field of 0 and 3 T.

Atomic line	Magnetic field			
	0 T		3 T	
	At %	Ratio	At %	Ratio
Fe K	0.52	1	0.62	1
Co K	0.76	1.5	0.79	1.3
C K	29.7		23.6	
O K	16.5		13.2	
Cu K	52.6		61.8	

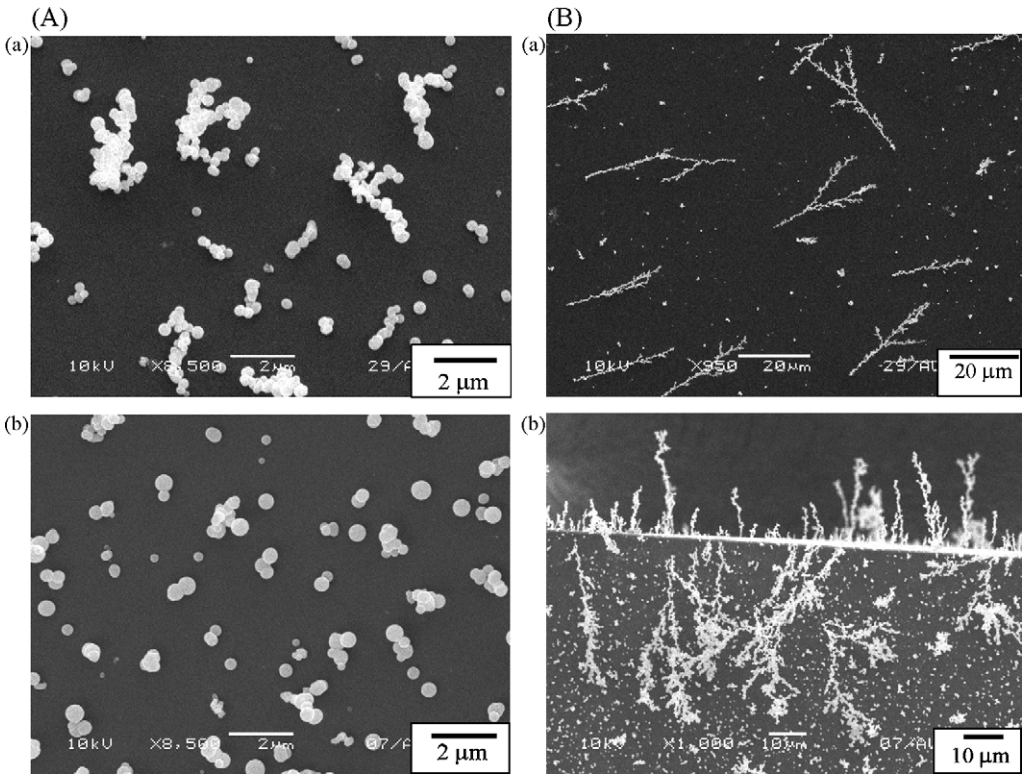

Fig. 8. (A) SEM images of sedimentary aerosol particles produced from a gaseous mixture of $Fe(CO)_5$ (0.4 Torr) and $Co(CO)_3NO$ (2.4 Torr) under light irradiation for (a) 7 and (b) 60 min. Original magnification of SEM, (a) and (b) 8500×. (B) SEM images of particle wires produced from a gaseous mixture of $Fe(CO)_5$ (0.4 Torr) and $Co(CO)_3NO$ (2.4 Torr) under light irradiation for (a) 7 and (b) 60 min. Original magnification of SEM, (a) 950×, (b) 1000×.

directly or via a bridging >C=O group as in the structure of $Co_2(CO)_8$ [32–35]. Disappearance of the IR band of the bridging >C=O group and appearance of the bands in 1250–1650 cm^{-1} region ascribed to C—O bond coordinated to a metal atom strongly suggest that (1) Fe atom in $Fe(CO)_4$ which is produced from $Fe(CO)_5$ via photodecomposition [27,28] coordinates the O atom in Co—(C=O)—Co structure to form Co—C—O—Fe structure and to result in the shift of the C—O stretching vibrational frequency to 1250–1650 cm^{-1} region, and/or (2) under UV light irradiation, two CO groups in such chemical species as $Co_2(CO)_6NO$ (reaction (7)) form α-diketone structure, and the O atom in the diketone structure coordinates to Fe atom in $Fe(CO)_4$ to show the ν(CO) band at 1500–1530 cm^{-1} [36]. On oxidized aluminum surface, $Co_2(CO)_8$ was reported to produce carbonate species [37]. Monodentate carbonate of Co showed asymmetric CO stretching band at 1540–1420 cm^{-1} and symmetric CO stretching band at 1390–1330 cm^{-1}. The Cu substrate used in the present experiment is significantly oxidized, hence the carbonate structure may be produced from CO groups during photochemical surface reaction in the presence of Co and Fe atoms. Judging from the spectrum in Fig. 10, the CO bands due to several chemical structures may contribute to the 1250–1650 cm^{-1} region, and the chemical structures discussed above may be formed during the particle formation.

The depletion of the gaseous molecules was measured from the intensity change of FT-IR bands of gaseous molecules. The results are shown in Fig. 11. Molar ratio of $Co(CO)_3NO$ to $Fe(CO)_5$ molecules depleted over 60 min was ~1.8. This value was close to the atomic ratio in the sedimentary particles analyzed by SEM–EDS. Due to the photodecomposition of gaseous molecules, the number

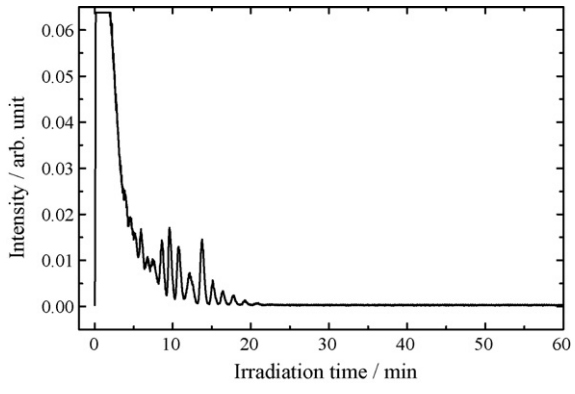

Fig. 9. He–Ne laser light intensity scattered by aerosol particles produced from a gaseous mixture of $Fe(CO)_5$ (0.4 Torr) and $Co(CO)_3NO$ (2.4 Torr) under light irradiation with a medium pressure mercury lamp.

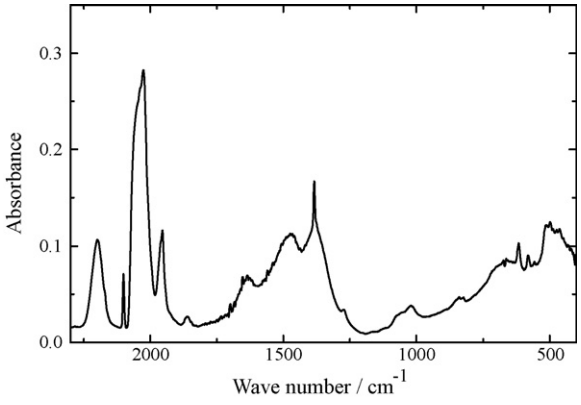

Fig. 10. FT-IR spectrum of sedimentary aerosol particles produced from a gaseous mixture of $Fe(CO)_5$ (0.4 Torr) and $Co(CO)_3NO$ (2.4 Torr) under light irradiation for 7 min.

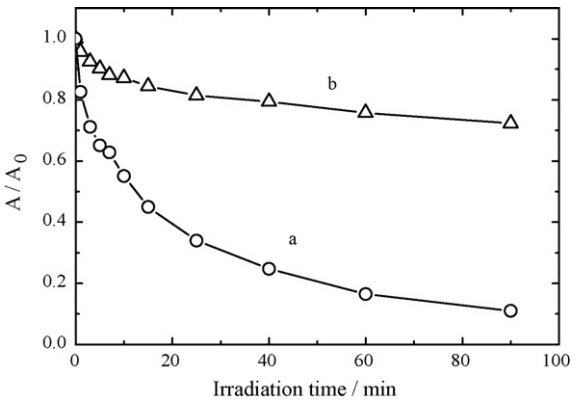

Fig. 11. Depletion (A/A_0) of (a) δ(Fe—C—O) band of $Fe(CO)_5$ and (b) ν(C≡O) band of $Co(CO)_3NO$ in a gaseous mixture of $Fe(CO)_5$ (0.4 Torr) and $Co(CO)_3NO$ (2.4 Torr) against irradiation time.

of $Co(CO)_3NO$ and $Fe(CO)_5$ molecules continued to decrease even after the completion of aerosol particle formation.

A gaseous mixture containing a little more $Fe(CO)_5$ (0.5 Torr) and a little less $Co(CO)_3NO$ (1.9 Torr) produced only sedimentary aerosol particles under UV light irradiation. FT-IR spectrum of the particles was essentially identical to the spectrum in Fig. 10, and SEM–EDS analysis revealed that the atomic ratio of Fe to Co atom was 1:1.3. The different atomic ratio of Fe to Co atom depending on the initial partial pressures of a gaseous mixture strongly suggested that the chemical structure of the aerosol particles was composed of several chemical structures involving Co and Fe atoms.

3.4. Magnetic field effect on chemical composition of sedimentary particles

Magnetic field effect on the chemical composition of the sedimentary aerosol particles was studied by SEM–EDS analysis. The result on the particles produced from a gaseous mixture of $Fe(CO)_5$ (0.4 Torr) and $Co(CO)_3NO$ (2.6 Torr) under a magnetic field of 3 T is tabulated in Table 3. The atomic ratio of Fe to Co atom was increased to 0.78 (1: 1.3) from 0.68 (1: 1.5) by the application of a magnetic field of 3 T, confirming that chemical reaction (8) was accelerated during aerosol particle formation by the application of a magnetic field as in the case where both the crystalline deposits and the particles were produced.

4. Conclusions

From a gaseous mixture of $Fe(CO)_5$ and $Co(CO)_3NO$, both the crystalline deposits with sizes of ∼5 and ∼18 μm and the spherical particles with a mean diameter of 0.3 μm were produced under UV light irradiation. From FT-IR spectra and SEM–EDS analysis, it was suggested that the chemical structure of the crystalline deposits was the one of $Fe_2(CO)_9$ being modified by involving Fe—(C=O)—Co bond. When the crystalline deposits were produced in the presence of a magnetic field of 5 T, they deposited on a substrate being aligned perpendicularly to the applied magnetic field due to the incorporation of divalent paramagnetic Co species. By decreasing a partial pressure of $Fe(CO)_5$ to 0.5 Torr in the gaseous mixture, only the spherical aerosol particles could be produced. Chemical composition of the particles was rich in Co species, and the atomic ratio of Fe to Co atom depended on the initial partial pressures of gaseous molecules. From the disappearance of bridging C=O band in the FT-IR spectra of the particles and the appearance of C—O bands coordinated to a metal atom, Fe atom in $Fe(CO)_4$ was suggested to be coordinated by the O atom in bridging C=O bond in Co—(C=O)—Co structure and/or in α-diketone structure which was formed from two CO groups in dicobalt species. Chemical compositions of the crystalline deposits and the spherical particles were influenced differently by the application of a magnetic field. Atomic ratio of Fe to Co atom decreased in the crystalline deposits whereas it increased in the spherical particles with increasing magnetic field up to 5 T. Linearly aggregated particles (i.e., particle wires) as long as 30 μm were produced on the front side of a glass plate placed at the bottom of the irradiation cell.

References

[1] M. Poliakoff, J.J. Turner, J. Chem. Soc. Dalton Trans. (1974) 2276.
[2] I.S. Butler, S. Kishner, K.R. Plowman, J. Mol. Struct. 43 (1978) 9.
[3] F.A. Cotton, J.M. Troup, J. Chem. Soc. Dalton Trans. (1974) 800.
[4] J. Knight, M.J. Mays, Chem. Commun. (1970) 1006.
[5] S.V. -Verdaguer, M.P. Morales, C.J. Serna, Mater. Lett. 35 (1998) 227.
[6] X.Q. Zhao, F. Zheng, Y. Liang, Z.Q. Hu, Y.B. Xu, Mater. Lett. 21 (1994) 285.
[7] T. Majima, Coord. Chem. Rev. 132 (1994) 141.
[8] S.V. -Verdaguer, O. Bomati, M.P. Morales, P.E. Di Nunzio, S. Martelli, Mater. Lett. 57 (2003) 1184.
[9] X.Q. Zhao, B.X. Liu, Y. Liang, Z.Q. Hu, J. Magn. Magn. Mater. 164 (1996) 401.
[10] T. Majima, T. Miyahara, K. Haneda, M. Takami, J. Photochem. Photobiol. A 80 (1994) 423.
[11] K.V.P.M. Shafi, A. Gedanken, R. Prozorov, J. Balogh, Chem. Mater. 10 (1998) 3445.
[12] H. Morita, J. Photopolym. Sci. Technol. 12 (1999) 95.
[13] H. Morita, M. Shimizu, J. Phys. Chem. 99 (1995) 7621.
[14] H. Morita, Y. Kimura, M. Kuwamura, T. Watanabe, J. Photochem. Photobiol. A 103 (1997) 27.
[15] H. Morita, K. Kanazawa, J. Photochem. Photobiol. A 112 (1998) 81.
[16] H. Morita, K. Semba, Z. Bastl, J. Pola, J. Photochem. Photobiol. A 116 (1998) 91.
[17] H. Morita, Y. Takeyasu, H. Okamura, H. Ishikawa, Sci. Technol. Adv. Mater. 7 (2006) 389.
[18] H. Morita, Y. Takeyasu, J. Šubrt, J. Photochem. Photobiol. A 197 (2008) 88.
[19] H. Morita, H. Ishikura, J. Photopolym. Sci. Technol. 18 (2005) 193.
[20] K. Abe, H. Morita, J. Photopolym. Sci. Technol. 19 (2006) 135.
[21] H. Morita, H. Sakano, C. Yamano, J. Photopolym. Sci. Technol. 20 (2007) 117.
[22] H. Morita, J. Photopolym. Sci. Technol. 21 (2008) 767.
[23] M. Bigorgne, J. Organometal. Chem. 24 (1970) 211.
[24] L.H. Jones, R.S. McDowell, M. Goldblatt, B.I. Swanson, J. Chem. Phys. 57 (1972) 2050.
[25] G. Bor, J. Organometal. Chem. 10 (1967) 343.
[26] L.H. Jones, R.S. McDowell, B.I. Swanson, J. Chem. Phys. 58 (1973) 3757.
[27] M. Poliakoff, J.J. Turner, J. Chem. Soc. Dalton Trans. (1973) 1351.
[28] M. Poliakoff, E. Weitz, Acc. Chem. Res. 20 (1987) 408.
[29] W. Wang, F. Chen, J. Lin, Y. She, J. Chem. Soc. Faraday Trans. 91 (1995) 847.
[30] M. Suwa, Y. Oshino, H. Watarai, H. Morita, A. Kasai, J. Šubrt, Sci. Technol. Adv. Mater. 9 (2008) 024215.
[31] K.S. Trauth, W.A. Burns, G. Berry, S.W. Reeve, J. Chem. Phys. 120 (2004) 4297.
[32] G.G. Sumner, H.P. Klug, L.E. Alexander, Acta Crystallogr. 17 (1964) 732.
[33] R.L. Sweany, T.L. Brown, Inorg. Chem. 16 (1977) 415.
[34] D.L. Lichtenberger, T.L. Brown, Inorg. Chem. 17 (1978) 1381.
[35] J.P. Kenny, R.B. King, H.F. Schaefer III, Inorg. Chem. 40 (2001) 900.
[36] K. Babić-Samardžija, S.P. Sovilj, N. Katsaros, J. Mol. Struct. 694 (2004) 165.
[37] M. Kurhinen, T.A. Pakkanen, Langmuir 14 (1998) 6907.